Molecular structure and ring tunneling of phenyl formate as observed by microwave spectroscopy and quantum chemistry

Lynn Ferres, Halima Mouhib, Wolfgang Stahl, Martin Schwell, Ha Vinh Lam Nguyen

Molecular structure and ring tunneling of phenyl formate as observed by microwave spectroscopy and quantum chemistry

Lynn Ferres,[a] Halima Mouhib,[a,b] Wolfgang Stahl,[a] Martin Schwell,[c] and Ha Vinh Lam Nguyen*[c]

[a] *Institute of Physical Chemistry, RWTH Aachen University, Landoltweg 2, D-52074 Aachen, Germany*

[b] *Laboratoire Modélisation et Simulation Multi Echelle, MSME UMR 8208 CNRS, Université Paris-Est, 5 bd. Descartes, F-77454 Marne-la-Vallée, France*

[c] *Laboratoire Interuniversitaire des Systèmes Atmosphériques (LISA), CNRS UMR 7583, Université Paris-Est Créteil, Université Paris Diderot, 61 avenue du Général de Gaulle, F-94010 Créteil cedex, France*

* Corresponding author: Dr. Ha Vinh Lam Nguyen

Email: lam.nguyen@lisa.u-pec.fr

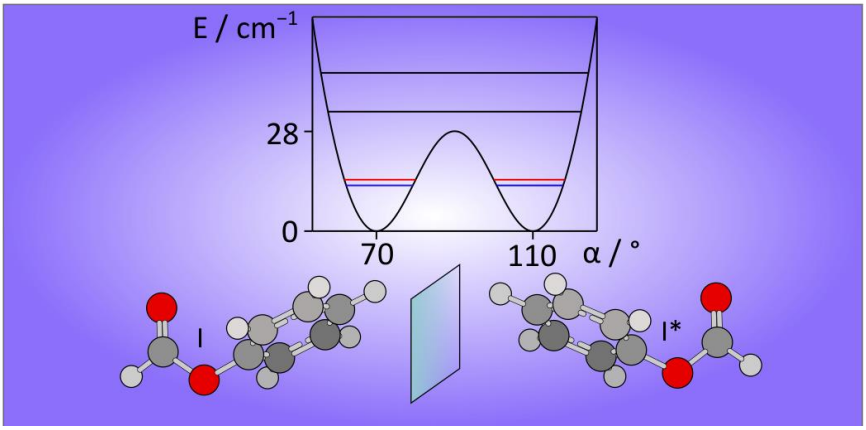

Molecular structure and ring tunneling of phenyl formate as observed by microwave spectroscopy and quantum chemistry

Phenyl formate has been investigated by molecular jet Fourier-transform microwave spectroscopy in the frequency range from 2 to 26.5 GHz. Quantum chemical calculations at the MP2/6-311++G(d,p) level of theory indicate that this molecule does not have a plane of symmetry at equilibrium, and that the phenyl ring performs a large amplitude tunneling motion from one side of the C_s configuration to the other. The tilt angle of the ring out of the H–(C=O)O plane is ±70° and the calculated tunneling barrier is only 28 cm^{-1}. The two lowest torsional states v_t = 0 and 1 are assigned in the experimental spectrum and fitted using the program *SPFIT/SPCAT*. The Coriolis splitting ΔE between these states is 46.2231(25) GHz, very close to the value of 48.24 GHz calculated using a simple two-top torsional Hamiltonian of the formate group and the phenyl ring.

Keywords: rotational spectroscopy; phenyl ring tunneling; double minima potential

1. Introduction

Phenyl formate (formic acid phenyl ester), $H(C=O)OC_6H_5$, with the structure illustrated in Figure 1, is a molecule of chemical, biological, quantum chemical, and spectroscopic interest.

Chemically, phenyl formate belongs to the class of small esters, which are widely used in organic chemistry as a reagent for the formylation of amines [1]. In addition, small esters contain a number of common odorant molecules. Many of these have been the object of our microwave studies, e.g. in Refs. [2-4], with a view toward determining dynamical and/or conformational properties that might correlate with processes involved in the sense of smell. Phenyl formate itself has a typical aromatic smell. It has been suggested in the process of olfaction that odorants may be carried by transport proteins, so-called odorant binding proteins, which can contain aromatic amino acids in their binding pocket such as tryptophan, phenylanaline, and tyrosine [5]. These amino acids could bind molecules such as phenyl formate and other aromatic odorants via π-π interactions [6]. Although under physiological conditions, conformations of aromatic compounds could be totally unrelated to the gas phase, it is important to understand the structure and dynamic of the isolated ligand without any influences from the environment. This is helpful to improve and develop force fields which can then be used to study the molecular dynamics of biological processes at a molecular scale.

Quantum chemically, the relatively small empirical formula of $C_7H_6O_2$ and the well-known planarity of the phenyl ring [7] and the formate group [8-10] suggest that structure optimizations carried out for phenyl formate are within the capabilities of our computational resources. Because it is not always possible to determine microwave spectroscopic structures using the traditional method by isotopic substitutions, the support of quantum chemistry is indispensable, as *ab initio* structures can be taken as references for a comparison of the experimental and calculated molecular parameters. As mentioned above, the orientation of the phenyl group is important in many biological processes, but it is difficult to predict.

Whenever possible, we tend to assume a plane of symmetry, i.e. the phenyl group is located in the plane formed by the heavy atoms of the formate group. This is the situation found for many phenyl ring containing molecules investigated by microwave spectroscopy so far, such as anisole [11], phenetole [12], acetophenone [13], benzoyl fluoride [14], and benzaldehyde [15]. On the other hand, in some cases phenyl rings are reported to tilt out of the plane spanned by its neighboring heavy atoms, e.g. in *cis* formanilide [16,17] and acetanilide [18]. Such tilt angle of a molecule fragment is not always easy to believe when it is based on the rather modest quantum chemistry calculations carried out in experimental spectroscopic laboratories, as e.g. in our investigations on allyl acetate [19]. As the present study shows, the phenyl group is also tilted out of the H(C=O)O plane in phenyl formate.

Spectroscopically, phenyl formate is a derivative of formic acid, where the proton in the acid group has been replaced by the much heavier phenyl group. When starting this work, we expected the spectrum of phenyl formate to be essentially that of a rigid-rotor with centrifugal distortion correction. However, as we shall see below, this simple rigid-rotor expectation turned out to be completely incorrect.

2. Quantum Chemical Calculations

All calculations were carried out at the MP2/6-311++G(d,p) level of theory with the *GAUSSIAN* program package [20]. For a conformational analysis, we varied the dihedral angles $\alpha = \angle(C_{13},O_{12},C_3,C_2)$ and $\beta = \angle(H_{14},C_{13},O_{12},C_3)$ in a grid of 10° (for atom numbering see Figure 1), corresponding to the rotation of the phenyl ring about the O_{12}–C_3 bond and the rotation of the formyl group HC=O about the C_{13}–O_{12} bond, respectively. The two-dimensional potential energy surface (2D-PES) depending on α and β revealed two stable conformers; each of which appears as four equivalent minima. Because of the planarity of both the phenyl ring and the formyl group, the geometries represented by (α,β), (α+180°,β),

(−α,−β), and (180°−α,−β) have the same potential energy, and only a quarter of the full 2D-PES calculations are necessary. The calculated energies were parameterized using a 2D Fourier expansion based on terms with the correct symmetry of the angles α and β. The coefficients from this parameterization are given in Table S-1 in the supplementary material. Using these Fourier coefficients, the 2D-PES was drawn as a contour plot illustrated in Figure 2.

If α is increased from 0° to 360° along the vertical lines at β = 0° or 180°, a series of four minima is found lying alternating slightly above and below the α = 90° and α = 270° lines. The *trans* conformer (conformer I), lying close to the β = 180° line, can be found in four different versions, I_a (α = 70.3°, β = 180.5°), I_a* (α = 109.7°, β = 179.5°), I_b (α = 250.3°, β = 180.5°), and I_b* (α = 289.7°, β = 179.5°) on the PES. The closer lying adjacent minima (I_a/I_a* and I_b/I_b* with $\Delta\alpha$ = 39.4°) are enantiomers, which are separated by a lower barrier of about 28 cm^{-1}, while the minima I_a/I_b and I_a*/I_b* with $\Delta\alpha$ = 180° arising from the 180° rotation of the phenyl ring are separated by a higher barrier of 726 cm^{-1}. This situation is depicted in Figure 3, where a one-dimensional "cut" along β = 180° of the PES is plotted. This cut is calculated by varying α from 0° to 360° at a starting value of β = 180°, while all molecular geometry parameters including β are optimized. The coefficients from this potential curve are given in Table S-2. All four versions of conformer I are shown in Figure 1. From a microwave spectroscopic point of view, they are identical and possess the same rotational constants. The geometry of conformer I_a is subsequently re-optimized under full geometry optimization, resulting in the rotational constants A = 3805.6 MHz, B = 1186.5 MHz, and C = 1039.9 MHz, and dipole moment components μ_a = 0.6 D, μ_b = −0.7 D, and μ_c = −1.3 D (in the principal axis system). The Cartesian coordinates are given in Table S-3 in the supplementary material.

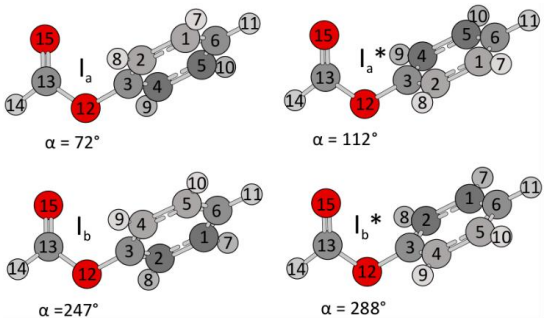

Figure 1: Four energetically equivalent minima of the most stable *trans* conformer I of phenyl formate. The structures were optimized at the MP2/6-311++G(d,p) level of theory. The dihedral angles $\alpha = \angle(C_{13},O_{12},C_3,C_2)$ are given. Note that the pairs I_a/I_a^* and I_b/I_b^* are enantiomers, while I_a and I_b as well as I_a^* and I_b^* can be transformed into each other by a rotation of 180° of the phenyl ring.

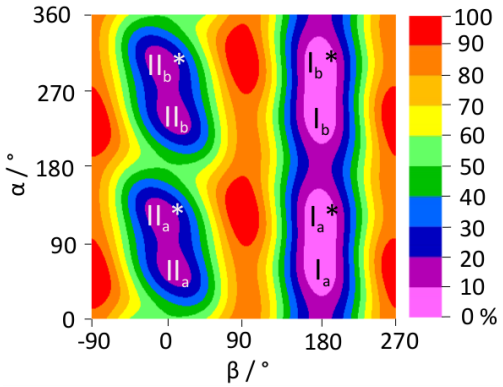

Figure 2: The potential energy surface of phenyl formate calculated at the MP2/6-311++G(d,p) level of theory depending on the dihedral angles $\alpha = \angle(C_{13},O_{12},C_3,C_2)$ and $\beta = \angle(H_{14},C_{13},O_{12},C_3)$. The color code indicates the energy (in per cent) relative to the energetically lowest conformations with E_{min} = –419.7514621 Hartree (0%). The energy maximum (100%) is E_{max} = –419.7327553 Hartree.

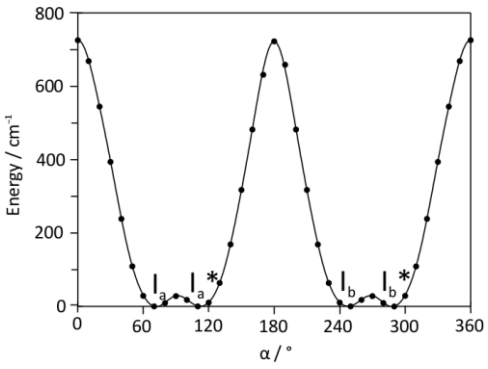

Figure 3: A one-dimensional "cut" of the potential surface in Figure 2 along the vertical line at β = 180° calculated by varying the dihedral angle α from 0° to 360° at a starting value of β = 180°. All molecular geometry parameters including β are optimized at the MP2/6-311++G(d,p) level of theory. The closer lying adjacent minima (with $\Delta\alpha \approx 40°$) are separated by a lower barrier of about 28 cm^{-1}, while the minima I_a/I_b and I_a*/I_b* (with $\Delta\alpha = 180°$) arising from the 180° rotation of the phenyl ring are separated by a higher barrier of 726 cm^{-1}.

The dihedral angle α of the minima in Figure 1 is not 0° as expected for C_s symmetry, i.e. the phenyl ring does not share a plane of symmetry with the H–(C=O)O frame. The tilt angle is ±70°, resulting in double minimum potentials within the regions α = (60°–120°) and (240°–300°) (see also Figure 3). A similar tilt angle out of the (C=O)O plane was found for the isopropenyl group in isopropenyl acetate [21]. Another molecule with a double minimum potential is *cis*-formanilide. The phenyl group is rotated by 35° out of the plane containing the pseudo-peptidic group. The barrier to planarity is 152 cm^{-1} [16]. A further example is acetanilide, which exists simultaneously as a planar and non-planar conformation. The non-planar compound has a phenyl ring tilted by 59° out of the C–(C=O)N plane, with almost exactly the same tunneling barrier of 151 cm^{-1} [18] as in the case of *cis*-formanilide.

The barriers of 28 cm^{-1} separating I_a and I_a* as well as I_b and I_b* are very small compared to those found in *cis*-formanilide and acetanilide. Tunneling of the phenyl ring is therefore very probable. In spite of these quantum chemistry indications of tunneling trouble, we still

began our spectroscopic analysis, as described in Section 3, under the assumption that this effect could be completely ignored because of the weight of the phenyl ring. When all attempts at obtaining a good rigid-rotor fit for the spectral measurements failed, we looked again at our quantum chemistry calculations. This will be discussed in detail in Section 3 and 4.

The *cis* conformer (conformer II), lying along the β = 0° line, can also be found in four different versions II_a (α = 57.9°, β = 5.7°), II_a*(α = 122.2°, β = 354.3°), II_b (α = 237.9°, β = 5.7°), and II_b* (α = 302.2°, β = 354.3°) on the PES with similar α value as that of conformer I for each version. The geometry of conformer II_a is re-optimized under full geometry relaxation, resulting in the rotational constants A = 4.8859 GHz, B = 0.9782 GHz, and C = 0.8438 GHz, dipole moment components μ_a = −4.53 D, μ_b = 0.82 D, and μ_c = 1.37 D, and (α,β) = (60.5°, 5.6°). It is noteworthy that these angles are slightly different from those obtained from the 2D-PES. The Cartesian coordinates are also given in Table S-3 in the supplementary material. The *cis* conformer is much higher in energy than the *trans* conformer (7.96 kJ/mol). This is in agreement with the results from our previous investigations on esters [22-24]. Therefore, we do not expect to observe this conformer under our molecular jet conditions, where the rotational temperature is very low (approximately 2 K), and only focus on the *trans* conformer in what following. Notably, we define *trans* conformations as in Figure 1, where the phenyl group is in *trans* position to the proton of the formate group.

3. Microwave spectroscopy

3.1. Measurement

For all measurements we used a molecular jet Fourier transform microwave spectrometer operating in the frequency range from 2 to 26.5 GHz [25]. Phenyl formate with a purity of 95% was purchased from Alfa Aesar, Kandel, Germany, and used without further purification. The substance was soaked on a pipe cleaner as carrier material, which was

inserted close to the nozzle. A helium stream with a pressure of 3 bar was flown over the sample and the resulting phenyl formate-helium mixture was expanded through a pulsed nozzle into the vacuum chamber.

The measurements were carried out first in a rapid scan mode between 8 and 16 GHz, where overlapping spectral segments were recorded with a step size of 0.25 MHz and 50 coadded decays for each spectrum. All lines from the scans were remeasured at higher resolution, where they appear as doublets due to the Doppler effect. The average value of all line widths is 20 kHz; the measurement accuracy is therefore 2 kHz.

3.2. Spectral assignment of the ground state $v_t = 0$

The calculated dipole moment components of the *trans* conformer given in Section 2 suggest that all *a*-, *b*-, and *c*-type transitions are present in the microwave spectrum. We first searched for *a*-type transitions in the broadband scan using a theoretical rigid-rotor spectrum predicted with the rotational constants also given in Section 2, because these transitions follow typical patterns which can be often recognized readily. Some lines following *a*-type selection rules could be easily identified. The first fit attempts were made with the program *XIAM* in its rigid-rotor mode [26]. Surprisingly, the assigned transitions could not be fitted well and the root-mean-square (rms) deviation was up to 3 MHz. Including the quartic centrifugal distortion constants in the fit did not decrease the rms deviation, and these parameters could not be determined well. This is strange, because rms deviations close to measurement accuracy can often be achieved in the fits of other rigid-rotor molecules [27-30]. Because of the typical *a*-type pattern in the microwave spectrum, we were quite confident that these assignments were correct. Using the rotational constants of the preliminary fit, we were able to assign also *b*- and *c*-type transitions by comparing the predicted and experimental spectrum. However, all attemps to reduce the rms deviation failed.

As mentioned in Section 2, it is very probable that some state other than the ground state is populated in our 2 K molecular jet, which comes from the effect of ring tunneling. The primary support for the existence of a low-lying state just above the $v_t = 0$ ground state is the fact that after a thorough assignment of recorded lines, a considerable number of transitions remained unassigned in the spectrum. They are much weaker than the assigned transitions, but on the other hand already quite strong that they are unlikely from the ^{13}C isotopologues. This low-lying state would then be a plausible candidate for a perturbation partner of the ground state. Assuming good thermal equilibrium in the jet, the intensity of the lines from this extra state suggests that it lies only about 10 cm^{-1} above the ground state, which in turn suggests that it is some tunneling component arising from the phenyl ring. We thus decided to calculate the eigenvalues of the four lowest energy levels that would occur from our potential energy curve given in Figure 3 in an attempt to determine whether this assumption is correct.

3.3. Calculations of low-lying tunneling states

The torsion of the phenyl ring against the formate group might cause low-lying excited torsional states which could be observed in the experiment. In order to estimate the energy separation between the $v_t = 0$ and 1 states and the ratio of the population numbers of both states under our experimental conditions, we made a simple model of two rigid tops rotating against each other.

We used the Hamiltonian (in cm^{-1} units)

$$\widehat{H} = -F\frac{d^2}{d\alpha^2} + V_0 + \sum_{n=1}^{7} V_{2n}\cos 2n\alpha$$

with the effective torsional constant $F = \frac{h}{8\pi^2 Ic} = 0.35101$ cm^{-1}. Here, c is the speed of light and $I = \frac{I_p I_f}{I_p + I_f} = 48.027$ uÅ^2 the effective moment of inertia calculated from the moments of inertia of the phenyl group $I_p = 102.738$ uÅ^2 and the formate group $I_f = 90.186$ uÅ^2. Both

of them refer to a rotation about the common torsional axis O_{12}–C_3 by the dihedral angle α. For the potential terms V_2, V_4, …, V_{14} we use the values 341.00, 115.29, 4.15, 10.03, 2.68, 3.27, and 0.53 cm^{-1}, respectively, derived from the parameterized potential curve given in Figure 3. The potential offset was chosen to be V_0 = 247.79 cm^{-1}, so that all potential minima are located at 0 cm^{-1}. The energy eigenvalues were obtained by a direct diagonalization of the Hamilton matrix set up in the plane wave basis $\psi_m = \frac{1}{\sqrt{2\pi}} e^{im\alpha}$ with m ∈{0, ±1, ±2, …}. The matrix was truncated at $|m|$ = 50, corresponding to a size of 101∗101, where convergence for the lowest energy levels in the kHz range was achieved.

The lowest energy levels are at 12.819 (0), 14.429 (1), 33.484 (2), and 44.344 cm^{-1} (3); all of them doubly degenerate. The torsional v_t quantum numbers are given in parentheses. The degeneracy arises from the fact that the potential function consists of a pair of double minimum potentials (see Figure 3) separated from each other by high potential walls of 726 cm^{-1}. No tunneling across these walls is observed and the energy levels remain degenerated. The potential functions in the range from 55 to 125° along with the lowest torsional levels are shown in Figure 4.

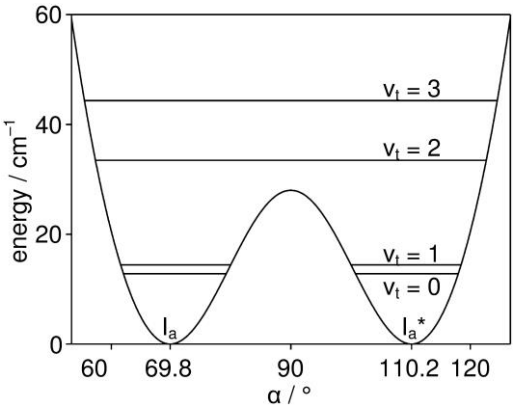

Figure 4: An enlargement in the range of 55 to 125° of the potential energy curve given in Figure 3, describing the torsion of the phenyl ring against the formate group by varying the angle α. Horizontal lines indicate the lowest torsional energy levels v_t = 0, 1, 2, 3, which are doubly degenerated.

The v_t : 1-0 difference is only 1.610 cm^{-1} or 48.24 GHz. This enables us to estimate the N_1/N_0 population ratio using the Boltzmann distribution $\frac{N_1}{N_0} = \exp\left(-\frac{\Delta E}{kT}\right)$ with the Boltzmann constant *k* and the temperature *T*. If we assume that the torsional temperature is in the same temperature range of 1 – 2 K as the rotational temperature in our jet, the estimated population of the excited state $v_t = 1$ is from 9.9 to 31.4 % with respect to the ground state $v_t = 0$.

3.4. Fits of the ground state $v_t = 0$

At this point, it is convincing that the low-lying $v_t = 1$ tunneling state is still populated in the jet-cooled spectrum that perturbs the ground state spectrum. We thus switched to the program *SPFIT/SPCAT* [31], available at the PROSPE website [32], which allows the user to choose Coriolis interaction terms for use in the fitting Hamiltonian. This feature allowed us to experiment with a number of tunneling parameters and centrifugal distortion corrections. At the beginning, the *SPFIT/SPCAT* program did not provide a better rms deviation than the *XIAM* program (close to 3 MHz). However, with gradually increasing number of parameters, especially by including the tunneling parameters *E*, E_J, F_{bc}, F_{ac}, and five sextic centrifugal distortion constants, among them the momentum cross terms F_{bc} and F_{ac} were essential to improve the fit, the situation improved. Molecular parameters were determined more accurately and rms deviation decreased to 3.7 kHz in a fit including 111 $v_t = 0$ rotational transitions with $J \leq 13$ and $K_a \leq 2$. The fitted parameters of this fit are given as Fit 0, $K_a \leq 2$ in Table 1.

Including eleven *a*-type *R*-branch lines with $K_a = 3$ and six further transitions with $J \geq 10$ in the fit increased the rms deviation to 14.8 kHz. The fitted parameters of this fit consisting of 128 lines are also collected as Fit 0, $K_a \leq 3$ in Table 1. A list of all fitted transitions is given in Table S-4; the $K_a = 3$ lines are marked by asterisks. Attemps to improve the situation for these transitions by including more parameters were not successful.

3.5. Global fits of the $v_t = 0$ and $v_t = 1$ states

After the $v_t = 0$ transitions were reasonably fitted using the program *SPFIT/SPCAT*, we found that many weaker lines with intensity of about 1/5 to 1/10 are located close to the most intense $v_t = 0$ lines (see Figure 5). From our previous investigation on pinacolone [33], we know that the low-lying $v_t = 1$ excited state, if still populated in the jet-cooled spectrum, is not far separated from the ground state. From the intensity calculations described in Section 3.3., the intensity of those weaker lines is in the correct order of magnitude as that predicted from the calculations. Therefore, we tried to assign these lines to the $v_t = 1$ excited state transitions of the same quantum numbers as those of the closest neiboring intense lines and could identify 33 lines. The global fit including 128 ground state $v_t = 0$ lines and 33 $v_t = 1$ lines has a rms deviation of 54.5 kHz. We used the effective Hamiltonian

$$H = \sum_{v=0}^{1} |v\rangle(H_r^v + H_\Delta^v)\langle v| + (|0\rangle\langle 1| + |1\rangle\langle 0|)H_c$$

where $|0\rangle$ and $|1\rangle$ represent the symmetric and the antisymmetric torsional state, respectively. The operator

$$\begin{aligned} H_r^v \quad &= A_v J_a^2 + B_v J_b^2 + C_v J_c^2 \\ &- \Delta_{J,v} J^4 - \Delta_{JK,v} J^2 J_a^2 - \Delta_{K,v} J_a^4 - \delta_{J,v} J^2 (J_+^2 + J_-^2) - \tfrac{1}{2}\delta_{K,v}[J_a^2, (J_+^2 + J_-^2)]_+ \\ &+ H_{J,v} J^6 + H_{JK,v} J^4 J_a^2 + H_{KJ,v} J^2 J_a^4 + H_{K,v} J_a^6 + h_{J,v} J^4 (J_+^2 + J_-^2) + \tfrac{1}{2} h_{JK,v} J^2 [J_a^2, (J_+^2 + J_-^2)]_+ \end{aligned}$$

with $J_\pm = J_b \pm iJ_c$ and the anti-commutator $[\dots, \dots]_+$ includes the overall rotation and the quartic and sextic centrifugal distortion terms of Watson's A reduction in the I^r representation. The rotational constants as well as the quartic and sextic centrifugal distortion constants depend on the torsional state *v*.

The torsional splitting between the $|0\rangle$ and the $|1\rangle$ energy levels and its *J* dependence is expressed by the operator

$$H_\Delta^v = v(E + E_J J^2).$$

Finally, the Coriolis operator connecting the $|0\rangle$ and the $|1\rangle$ torsional state is given by

$$\begin{aligned} H_c \quad &= G_a J_a + G_b J_b \\ &+ F_{ac}(J_a J_c + J_c J_a) + F_{bc}(J_b J_c + J_c J_b) \\ &+ F_{acK} J_a^2 (J_a J_c + J_c J_a) + F_{bcK} J_a^2 (J_b J_c + J_c J_b). \end{aligned}$$

The fitted molecular parameters are summerized as Fit 01 in Table 1 and in Table S-5 in the supplementary material. The frequencies along with their residues are collected in Table S-4 and S-6. It is remarkable that a nearly complete set of quartic and sextic centrifugal distortion constants are needed separately for the excited state in spite of the very limited number of lines in the fit. Including more parameters did not help to reduce the rms deviation.

4. Discussion

The ground state fit including 128 lines given as Fit 0 in Table 1 has a rms deviation of 14.8 kHz. This deviation, which is seven times the measurement accuracy, is already quite succesful comparing to the fit using only a rigid-rotor model. The key parameters are F_{bc} and F_{ac}, which are associated with the v_t-off-diagonal matrix elements of the operators $\{J_b,J_c\}$ and $\{J_a,J_c\}$, respectively, with their large values of –33.6 and 163.3 MHz. The Coriolis splitting ΔE of 43.4233(80) GHz is quite close to the estimated value of 48.27 GHz (see Section 3.4).

Though the fitted value of ΔE in the global Fit 01 is even closer to the calculated one, the rms deviation of 54.5 kHz of this fit is unreasonably large comparing to the measurement accuracy of 2 kHz or to that of the ground state Fit 0. A large number of centrifugal distortion constants are needed for the fit, which is quite unusual for a fit of only low-J and K transitions (i.e. $J \leq 13$, $K_a \leq 3$). The difference between the rotational constants A, B, and C of the ground and the excited state is remarkable. Also almost all centrifugal distortion constants are in different orders of magnitude. In other molecules, where similar tunneling problems were reported, e.g. benzyl alcohol [34], *cis*-formanilide [16], and acetanilide [18], these differences found for the rotational constants were less significant, and the same set of centrifugal distortion constants could be used for both states.

We believe that all these problems arise because the tunneling motion of phenyl format is not correcty captured by the present set of fitted parameters and because of the

limited number of excited state lines, the relatively low tunneling barrier, as well as the large tilt angle of the phenyl ring (see Section 2). Assigning and including more lines of the $v_t = 1$ excited state might improve the fit quality. However, the measurements of these transitions under our jet-cooled conditions are rather limited because of the low line intensity and yet unreliable prediction. After excluding all assigned $v_t = 0$ and $v_t = 1$ lines, no intense lines remained in the broadband scan, as shown in Figure 5.

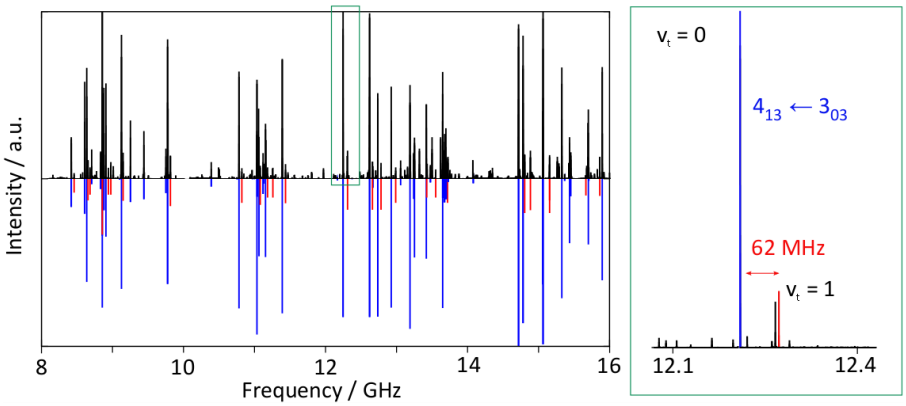

Figure 5: Left hand side: A section from 8 – 16 GHz of the broadband scan (upper trace) of phenyl formate compared to the theoretical spectrum reproduced with the *SPFIT/SPCAT* program (lower trace). Transitions of the $v_t = 0$ ground state are marked in blue, those of the $v_t = 1$ excited state in red. Right hand side: A section from 12.1 – 12.4 GHz of the broadband scan showing the $v_t = 0$ and $v_t = 1$ components of the $4_{13} \leftarrow 3_{03}$ transition with a torsional splitting of 62 MHz.

References

[1] H. Yale, J. Org. Chem. 36 (1971) 3238.

[2] H. Mouhib, D. Jelisavac, L.W. Sutikdja, E. Isaak, W. Stahl, J. Phys. Chem. A 115 (2011) 118.

[3] L. Sutikdja, W. Stahl, V. Sironneau, H.V.L. Nguyen, I. Kleiner, Chem. Phys. Lett. 663 (2016) 145.

[4] L.W. Sutikdja, D. Jelisavac, W. Stahl, I. Kleiner, Mol. Phys. 110 (2012) 2883.

[5] S. Firestein, Nature 413 (2001) 211.

[6] K. Herrmann, Alkaloidhaltige Genussmittel, Gewürze, Kochsalz, Springer (1979) 632.

[7] D. Moran, A.C. Simmonett, F.E. Leach, W.D. Allen, P.v.R. Schleyer, H.F. Schaefer, J. Am. Chem. Soc. 128 (2006) 9342.

[8] R. F. Curl, J. Chem. Phys. 30 (1959) 1529.

[9] W. Pyckhout, C.V. Alsenoy, H.J. Geise, J. Mol. Struct. 147 (1986) 85.

[10] G.I.L. Jones, D.G. Lister, N.L. Owen, J. Chem. Soc. Faraday Trans. 2, 71 (1975) 1330.

[11] M. Onda, A. Toda, S. Mori, I. Yamaguchi, J. Mol. Struct. 144 (1986) 47.

[12] L. Ferres, W. Stahl, H.V.L. Nguyen, Mol. Phys. 114 (2016) 2788.

[13] M. Onda, Y. Kohama, K. Suga, I. Yamaguchi, J. Mol. Struct. 442 (1998) 19.

[14] R.K. Kakar, J. Chem. Phys. 56 (1972) 1189.

[15] R.K. Kakar, E.A. Rinehart, C.R. Quade, T. Kojima, J. Chem. Phys. 52 (1970) 3803.

[16] S. Blanco, J.C. Lopez, A. Lesarri, W. Caminati, J.L. Alonso, Mol. Phys. 103 (2005) 1473.

[17] J.-R.A. Moreno, D. Petitprez, T.R. Huet, Chem. Phys. Lett. 419 (2006) 411.

[18] C. Cabezas, M. Varela, W. Caminati, S. Mata, J.C. López, J.L. Alonso, J. Mol. Spectrosc. 268 (2011) 42.

[19] H.V.L. Nguyen, H. Mouhib, W. Stahl, I. Kleiner, Mol. Phys. 108 (2010) 763.

[20] M.J. Frisch, G.W. Trucks, H.B. Schlegel, G.E. Scuseria, M.A. Robb, J.R. Cheeseman, G. Scalmani, V. Barone, B. Mennucci, G.A. Petersson, H. Nakatsuji, M. Caricato, X. Li, H.P. Hratchian, A.F. Izmaylov, J. Bloino, G. Zheng, J.L. Sonnenberg, M. Hada, M. Ehara, K. Toyota, R. Fukuda, J. Hasegawa, M. Ishida, T. Nakajima, Y. Honda, O. Kitao, H. Nakai, T. Vreven, J.A. Montgomery, Jr., J.E. Peralta, F. Ogliaro, M. Bearpark, J.J. Heyd, E. Brothers, K.N. Kudin, V.N. Staroverov, R. Kobayashi, J. Normand, K. Raghavachari, A. Rendell, J.C. Burant, S.S. Iyengar, J. Tomasi, M. Cossi, N. Rega, J.M. Millam, M. Klene, J.E. Knox, J.B. Cross, V. Bakken, C. Adamo, J. Jaramillo, R. Gomperts, R.E. Stratmann, O. Yazyev, A.J. Austin, R. Cammi, C. Pomelli, J.W. Ochterski, R.L. Martin, K. Morokuma, V.G. Zakrzewski,

G.A. Voth, P. Salvador, J.J. Dannenberg, S. Dapprich, A.D. Daniels, O. Farkas, J.B. Foresman, J.V. Ortiz, J. Cioslowski and D.J. Fox, Gaussian 09, Revision A.02, Gaussian, Inc., Wallingford CT, 2009.

[21] H.V.L. Nguyen, W. Stahl, J. Mol. Spectrosc. 264 (2010) 120.

[22] D. Jelisavac, D.C. Cortés Gómez, H.V.L. Nguyen, L.W. Sutikdja, W. Stahl, I. Kleiner, J. Mol. Spectrosc. 257 (2009) 111.

[23] H.V.L. Nguyen, A. Jabri, V. Van, W. Stahl, J. Phys. Chem. A 118 (2014) 12130.

[24] A. Jabri, V. Van, H.V.L. Nguyen, W. Stahl, I. Kleiner, ChemPhysChem 17 (2016), 2660.

[25] J.-U. Grabow, W. Stahl, H. Dreizler, Rev. Sci. Instrum. 67 (1996) 4072.

[26] H. Hartwig, H. Dreizler, Z. Naturforsch. 51a (1996) 923.

[27] V. Van, C. Dindic, W. Stahl, H.V.L. Nguyen, ChemPhysChem 16 (2015) 291.

[28] R. Kannengießer, W. Stahl, H.V.L. Nguyen, W.C. Bailey, J. Mol. Spectrosc. 317 (2015) 50.

[29] V. Van, W. Stahl, H.V.L. Nguyen, J. Mol. Struct. 1123 (2016) 24.

[30] R. Kannengießer, W. Stahl, H.V.L. Nguyen, J. Phys. Chem. A 120 (2016) 5979.

[31] H.M. Pickett, J.Mol. Spectrosc. 148 (1991) 371.

[32] http://www.ifpan.edu.pl/~kisiel/prospe.htm.

[33] Y. Zhao, H.V.L. Nguyen, W. Stahl, J.T. Hougen, J. Mol. Spectrosc. 318 (2015) 91.

[34] K.A. Utzaz, R.K. Bohn, J.A. Montgomery Jr, H.H. Michels, W. Caminati, J. Phys. Chem. A 114 (2010) 6913.

Acknowledgements

We thank the Land Nordrhein-Westfalen and the Université Paris-Est Créteil for funds as well as the IT Center of the RWTH Aachen University for free computing time. H.M. thanks the Excellence Initiative grants of the German federal and state governments (StUpPD_209_15).

Tables

Table1. Molecular parameters of phenyl formate from the fits using the *SPFIT/SPCAT* program and from quantum chemical calculations.

Par.[a]	**Unit**	**Fit 0** $K_a \leq 2$	**Fit 0** $K_a \leq 3$	**Fit 01** $\mathbf{v_t = 0}$	**Fit 01** $\mathbf{v_t = 1}$	**Calc.**[b]
A	MHz	3848.257(68)	3838.160(12)	3899.83(22)	3836.97(22)	3733.074
B	MHz	1167.241(86)	1157.037(12)	1181.770(24)	1161.371(17)	1188.168
C	MHz	1045.998(94)	1034.813(15)	1047.539(11)	1045.8128(99)	1058.306
Δ_J	kHz	–0.299(19)	0.8837(38)	1.9010(34)	14.5174(69)	0.2530
Δ_{JK}	MHz	0.2352(33)	0.10513(31)	0.70918(59)	–0.48479(62)	0.002649
Δ_K	MHz	1.326(23)	0.9830(37)	–3.3248(30)	–2.086(16)	–0.0004919
δ_J	kHz	1.521(68)	1.5880(14)	1.3566(32)	–3.4393(22)	–0.04523
δ_K	kHz	572.8(38)	288.5(11)	–65.83(39)	1.08(51)	–0.1168
H_J	Hz	–5.693(29)	–9.1462(96)			$-0.1499\cdot10^{-3}$
H_{JK}	kHz	0.6045(68)	0.36501(35)	–0.90338(81)	-0.7635(44)	$0.8028\cdot10^{-4}$
H_K	MHz	–0.3113(52)	–0.21843(77)	0.57522(69)	0.4811(30)	$0.3106\cdot10^{-6}$
H_{KJ}	kHz	0.01457(25)	1.6060(55)	–41.872(42)	34.950(69)	$-0.3908\cdot10^{-3}$
h_J	Hz			–3.9443(24)		$-0.1325\cdot10^{-3}$
h_{JK}	kHz	–0.6214(49)	–1.2453(12)		3.5970(14)	$-0.3301\cdot10^{-4}$
E	GHz	33.651(97)	43.4233(80)	46.2231(25)		48.27[c]
E_J	MHz	6.031(89)	16.670(12)			
F_{bc}	MHz	–21.70(19)	– 34.562(16)	34.3872(95)		
F_{ac}	MHz	158.034(91)	163.335(30)	168.201(19)		
F_{bcK}	MHz			1.8247(22)		
F_{acK}	MHz			– 3.8755(32)		
G_a	GHz			1.3164(38)		
G_b	GHz			0.64351(67)		
N[d]		111	128	128	33	
rms[e]	kHz	3.7	14.8	54.5		

[a] All parameters refer to the principal axis system. Watson's A reduction and I^r representation were used. [b] Anharmonic frequency calculations at the MP2/6-311++G(d,p) level of theory. The rotational constants are the B_0 ground state constants and are different from the B_e equilibrium constants given in Section 2. [c] See Section 3.4. [d] Number of lines. [e] Root-mean-square deviation of the fit.